

Ion-Wave Instabilities in Mercury-Vapor Plasma

H. TANACA, A. HIROSE, AND M. KOGANEI

Institute of Materials Science and Engineering, Yokohama National University, Yokohama, Japan

(Received 3 February 1967)

The Landau dispersion equation $2k^2 = k_{De}^2 Z'(\zeta_e) + k_{Di}^2 Z'(\zeta_i)$ is studied experimentally for $\omega = \omega_r + i\omega_i$, where $\omega_i = 0$ determines the stable-unstable boundary of ion waves, k_{De} and k_{Di} are the electron and ion Debye wave numbers, and $Z(\zeta)$ is the plasma dispersion function. The decrease of the phase velocity with the frequency predicted by dispersion relation is observed for the spontaneously excited ion waves in the mercury-vapor discharge. The cutoff frequency beyond which no ion waves appear is also observed. The cutoff frequency increases with the electron drift velocity in the plasma. The dependence of the cutoff frequency on the electron drift is explained by the ion-wave instability in a two-Maxwellian-component plasma. One-way propagation of externally excited ion waves is also shown.

I. INTRODUCTION

SINCE the beginning of the study of plasma physics, it has been widely known that certain kinds of electrostatic waves (such as plasma oscillations) can be sustained in a plasma.¹ So-called ion waves in which momentum transfer is mainly due to ions are a typical example in the low-frequency region. According to the fluid model of a plasma, the dispersion relation of the ion waves is given by²

$$\omega_{pi}^2 / (\omega^2 - \gamma_i k^2 \omega_{pi}^2 / k_{Di}^2) = 1 + k_{De}^2 / \gamma_e k^2, \quad (1)$$

where ω_{pi} is the ion plasma frequency, k_{De} and k_{Di} the electron and ion Debye wave numbers, respectively, and γ_e, γ_i are the electron and ion compressional coefficients, respectively. These waves are sustained by Coulomb forces resulting from a slight deviation from charge neutrality in the plasma. Since the ions and electrons move in phase, the motion of the plasma is, in a certain sense, similar to the ambipolar diffusion in a nonuniform plasma.³ If $k \ll k_{De}$, i.e., for long wavelength, Eq. (1) is reduced to

$$\omega^2 / k^2 = (\gamma_e T_e + \gamma_i T_i) / M, \quad (2)$$

where M is the ion mass and T_e and T_i the electron and ion temperatures (eV). This relation determines the velocity of the ion acoustic waves.⁴

However, the fluid model does not predict the excitation and damping mechanism of the ion waves. In fact, only with kinetic theory can the effect of Landau damping⁵ of ion waves be described. Recently, ion wave instabilities have been discussed by several authors⁶⁻¹²

using kinetic theory. The Landau dispersion equation for longitudinal waves in a two-Maxwellian-component plasma is

$$2k^2 = k_{De}^2 Z'(\zeta_e) + k_{Di}^2 Z'(\zeta_i), \quad (3)$$

$$\zeta_e = [(\omega/k) - V] / \beta_e, \quad \zeta_i = \omega / k \beta_i,$$

where $Z(\zeta)$ is the plasma dispersion function, $Z'(\zeta)$ its derivative, β_e and β_i are the electron and ion thermal velocities and V is the relative drift velocity between ions and electrons. In the absence of electron drift, this equation reduces, with approximation of $|\zeta_e| \ll 1$ and $|\zeta_i| \gg 1$, to the ordinary dispersion relation Eq. (1) for the case of $\gamma_e = 1, \gamma_i = 3$. When Eq. (3) is solved for complex frequency $\omega = \omega_r + i\omega_i$, the imaginary part ω_i gives the growth or damping rate of the waves. Therefore the region of instability is determined from the condition $\omega_i = 0$. Taking the temperature ratio T_e/T_i as a parameter, the stable-unstable boundary can be expressed in terms of wave number k and drift velocity V . The essential character of the ion wave instability induced by the relative velocity between the two types of particles may be considered as a version of two-stream instability.¹³ From a mathematical point of view, it is equivalent to the Nyquist's criterion in automatic-control theory.¹⁴

Recently, we have experimentally observed the simple dispersion relation [Eq. (1)] without considering the theoretical effect of ion temperature.¹⁵ Also we have observed the existence of a cutoff frequency in the dispersion relation beyond which no spontaneous excitation of the waves appears.¹⁵ The dependence of cutoff frequency on electron drift has been explained by the drift instability of a two-Maxwellian-component plasma.¹⁶ In the present work, as an integration of our previous short papers, we report on the ion wave instabilities in mercury-vapor discharges with a more detailed analysis in terms of the kinetic theory of plasma, especially for the Landau dispersion equation [Eq. (3)]. In Sec. II the theoretical background of our experiment is briefly summarized. In Sec. III our

¹ I. L. Tonks and I. Langmuir, *Phys. Rev.* **33**, 195 (1929).

² L. Spitzer, Jr., *Physics of Fully Ionized Gases* (Interscience Publishers, Inc., New York, 1962).

³ J. F. Dennise and J. L. Delcroix, *Théorie des Ondes dans les Plasmas* (Dunod Cie., Paris, 1961).

⁴ Detailed literatures of the experiments of the ion acoustic waves are given by F. W. Crawford and R. M. Muhler, in *Proceedings of the Seventh International Conference on Ionization Phenomena in Gases*, Belgrade, 1965 (unpublished).

⁵ L. D. Landau, *J. Phys. (USSR)* **10**, 25 (1946).

⁶ O. Buneman, *Phys. Rev.* **115**, 503 (1959).

⁷ J. D. Jackson, *J. Nucl. Energy, Pt. C* **1**, 171 (1960).

⁸ E. A. Jackson, *Phys. Fluids* **3**, 786 (1960).

⁹ I. B. Bernstein and R. M. Kulsrud, *Phys. Fluids* **3**, 937 (1960).

¹⁰ B. D. Fried and R. W. Gould, *Phys. Fluids* **4**, 139 (1961).

¹¹ E. R. Harrison, *Proc. Phys. Soc. (London)* **80**, 432 (1962).

¹² D. G. Lominadze and K. N. Stepanov, *Zh. Tekhn. Fiz.* **35**, 449 (1965) [English transl.: *Soviet Phys.—Tech. Phys.* **10**, 352 (1965)].

¹³ D. Bohm and E. P. Gross, *Phys. Rev.* **75**, 1864 (1949).

¹⁴ H. Nyquist, *Bell System Tech. J.* **11**, 126 (1932).

¹⁵ H. Tanaca, M. Koganei, and A. Hirose, *Phys. Rev. Letters* **16**, 1079 (1966).

¹⁶ H. Tanaca, A. Hirose, and M. Koganei, *Phys. Letters* **23**, 679 (1966).

experimental arrangements for the mercury-vapor discharges are shown. In Sec. IV the experimental results on the dispersion of ion waves and the dependence of the cutoff on electron drift are presented. The one-way propagation of the waves is also shown. These results are in good agreement with the Landau dispersion equation. The detailed discussions omitted in the previous short papers are given in Sec. V.

II. THEORETICAL BACKGROUND

We assume a collisionless and uniform plasma with no external magnetic field. In the one-dimensional approach, the longitudinal waves are described by the Boltzmann-Vlasov and Poisson equations as follows¹⁷:

$$\partial f_e/\partial t + v\partial f_e/\partial Z - (eE/m)\partial f_e/\partial v = 0, \quad (4)$$

$$\partial f_i/\partial t + v\partial f_i/\partial Z + (eE/M)\partial f_i/\partial v = 0, \quad (5)$$

$$\frac{\partial E}{\partial z} = 4\pi e \int_{-\infty}^{\infty} (f_i - f_e) dv, \quad (6)$$

where ions are singly ionized. To linearize the above set of equations, we assume small perturbations in f_e and f_i , which are proportional to $\exp[i(kz - \omega t)]$. Then, after the Fourier-Laplace transformation, the equations can be solved as an initial-value problem. However, the dispersion relation is easily written even before the final solutions are obtained. Following Landau, the dispersion equation is given by

$$2k^2 = k_{De}^2 Z'(\zeta_e) + k_{Di}^2 Z'(\zeta_i) \quad (3)$$

for a two-Maxwellian-component plasma. In Eq. (3), Z' , the derivative of the plasma dispersion function, is defined by

$$Z'(\zeta) = \frac{2}{\sqrt{\pi}} \int_C \frac{x e^{-x^2}}{\zeta - x} dx, \quad (7)$$

where the integration path C is from $-\infty$ to $+\infty$ except for a small semicircle under the pole ζ .¹⁸ The numerical values of $Z(\zeta)$ and $Z'(\zeta)$ are tabulated in the book of Fried and Conte¹⁹ for $\zeta = (0 \pm i0) - (10 \pm i10)$ at 0.1 intervals.

Concerning the spontaneous excitation of ion waves in the discharge, we assume that the wave number k is real and the angular frequency ω , complex, with $\omega = \omega_r + i\omega_i$. Then, $\omega_i > 0$ represents growing waves and $\omega_i < 0$, damped waves. The stable-unstable boundary is determined by solving Eq. (3) for $\omega_i = 0$. Then Eq. (3) can be written as

$$2k^2/k_{De}^2 = Z'(\zeta_e) + (T_e/T_i)Z'(\zeta_i), \quad (8)$$

where one can see easily that the temperature ratio T_e/T_i is significant in the determination of the stable-

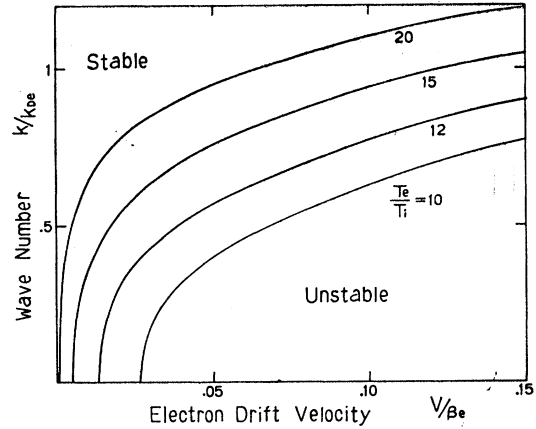


FIG. 1. Stable-unstable boundary as a function of T_e/T_i .

unstable boundary. According to Jackson,⁸ the stable-unstable boundary is obtained by graphically solving Eq. (8). Some examples of the boundary are shown in Fig. 1 in the case of rather a small drift velocity. The unstable region becomes larger as the temperature ratio T_e/T_i increases, because the effect of Landau damping due to the thermal motion of ions decreases. The theory predicts that stable-unstable boundary can be represented, in terms of the experiment, by the appearance of cutoff frequency or wave number beyond which no spontaneously excited waves are observed. Also, according to the theory such a cutoff wave number increases, at a constant temperature, with the electron drift velocity in our experimental range. The dependence of the cutoff wave number on the electron drift velocity is examined in the experiment, as is shown below.

It is worthwhile to show the relation between the two different forms of the dispersion relation as given in Eqs. (1) and (3). From the asymptotic expansion of $Z'(\zeta)$ it can be easily shown that¹¹

$$Z'(\zeta_e) \rightarrow -2 \quad \text{for } |\zeta_e| \ll 1, \quad (9)$$

$$Z'(\zeta_i) \rightarrow 1/\zeta_i^2 + 3/2\zeta_i^4 \approx 2/(2\zeta_i^2 - 3) \quad \text{for } |\zeta_i| \gg 1. \quad (10)$$

Substituting (9) and (10) into (8), one obtains

$$\omega_{pi}^2/[\omega^2 - 3k^2 T_i/M] = 1 + k_{De}^2/k^2. \quad (11)$$

Equation (11) is identical with Eq. (1) provided that $\gamma_e = 1$ and $\gamma_i = 3$. The assumption $|\zeta_e| \ll 1$ and $|\zeta_i| \gg 1$ means that the drift velocity is much smaller than the electron thermal velocity and the phase velocity of the waves is much larger than the ion thermal velocity. In such a case, the plasma kinetic theory in the one-dimensional approach gives the same result as the fluid model, where the density fluctuations of ions are adiabatic while those of electrons are isothermal. In our experiment, however, the phase velocity of the waves exceeds the ion thermal velocity by a factor of only 2 or 3, and

¹⁷ A. Vlasov, J. Phys. (USSR) **9**, 25 (1945).

¹⁸ P. M. Morse and H. Feshbach, *Methods of Theoretical Physics* (McGraw-Hill Book Company, Inc., New York, 1953).

¹⁹ B. D. Fried and S. D. Conte, *The Plasma Dispersion Function* (Academic Press Inc., New York, 1961).

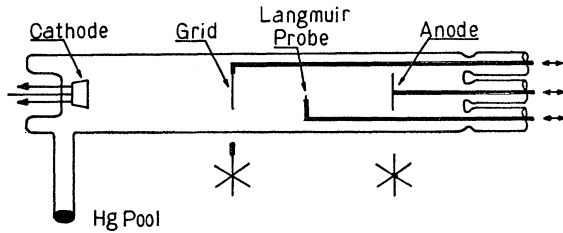


FIG. 2. Schematic diagram of the discharge tube.

therefore $|\zeta_i| \gg 1$ is not sufficiently satisfied, whereas $|\zeta_e| \ll 1$ is well satisfied.

We wish to add an important comment on the condition for a growing mode in our plasma. Because ω is complex in our case, the argument of the dispersion function Z must be complex, that is, $\zeta = \text{Re}\zeta + i\text{Im}\zeta$. As is easily derived from the definition of the function Z , $\text{Im}Z'(\zeta) \geq 0$ for $\text{Re}\zeta \leq 0$, respectively, whenever $\text{Im}\zeta > 0$, $\text{Im}\zeta > 0$ corresponds to the growing mode. In Eq. (8), since the left-hand side contains only a real term, the imaginary parts in the right-hand side should cancel each other. This requires, at least, that $\text{Im}Z'(\zeta_e)\text{Im}Z'(\zeta_i) < 0$. Taking into account our plasma state, where the electron drift velocity is higher than the phase velocity of ion waves, a necessary condition for a growing mode is expressed as $0 < \omega_r/k < V$, when $V > 0$. This implies one-way propagation of the ion waves; only the waves propagating in the direction of the electron drift are enhanced.

In the following sections, experimental results for the ion waves are compared with the Landau dispersion equation (8), in order to examine the relation between ion-wave instabilities and the cutoff-frequency dependence on the electron drift velocity.

III. EXPERIMENTAL ARRANGEMENTS

A diagram of the mercury-vapor discharge tube is shown in Fig. 2. The tube is 3.5 cm in diam and 25 cm in length. The maximum effective length of positive column is about 20 cm. An indirectly heated cathode, 7 mm in diam, is installed. The anode is composed of three tungsten wires (0.5 cm in diam and 15 mm in length) combined to form an "asterisk" anode. The surface of such an anode is much smaller than that of a usual disk anode. However, the maximum discharge current throughout our present experiments is less than 40 mA, and compared with the disk anode we can observe no distinct difference in the discharge states except for a slight increase in the voltage at the asterisk anode. The electric field in the plasma remains unchanged. Empirically we find that this particular shape of anode provides us with the most effective boundary for the ion waves.

A grid of the same shape and size which also acts as a boundary for ion waves is inserted into the positive column. It does not disturb the discharge parameters. In particular, the internal electric field on which the

electron drift velocity strongly depends is not changed. The grid is kept at the floating potential. A Langmuir probe movable both axially and azimuthally is installed. It has a cylindrical tungsten tip of 0.2 mm in diam and 3 mm in length.

The mercury pool of the tube is immersed in a thermostat to control the mercury-vapor pressure. In this way, the electron drift velocity in the plasma is varied.

Spontaneously excited ion waves between the asterisk anode and grid are observed for wide ranges of the anode-grid distance (0.3–5.0 cm) and discharge currents (3.0–30 mA). In order to examine the frequency spectra of the waves, the spectrum analysis is carried out by either a panoramic spectrum analyzer or a selective level meter.

The propagation of the waves is examined by a phase-sensitive detector which measures wavelength directly (Fig. 3). In earlier experimental work on the dispersive character of ion waves, the dependence of velocity on the wave number has not been observed,^{20,21} because the wavelength was presumed constant from geometrical considerations. In our experiment, however, this ambiguity is removed by the direct measurement of the wavelength, and the variation of velocity with wave number is clearly demonstrated.

Electron density is measured by the Langmuir probe and varies between 2×10^8 and $5 \times 10^9/\text{cm}^3$. More exactly, however, the density can be determined as a fitting parameter in the dispersion relation.

The electron temperature T_e is also measured by the probe. The value $T_e = 1.2 \pm 0.1$ (eV) is independent of electron density. We may expect that there is no significant difference between $T_{e\parallel}$ and $T_{e\perp}$ in the plasma because the internal electric field in the plasma is very small and there is no external magnetic field.

The ion temperature T_i , which is an important parameter in comparison with theory, is not measured directly in the experiment. As will be shown later, the ion temperature is of the order 0.1 eV.

The electron drift velocity is varied by controlling the mercury vapor pressure. The mercury vapor pressure p (mm of Hg) ranges from 3.4×10^{-4} to 2.7×10^{-3} in accordance with the temperature variation from 5 to 30°C. The internal electric field E (V/cm) in the plasma column is calculated from the average difference of space potentials in the plasma. We obtain $E \sim 0.01$,

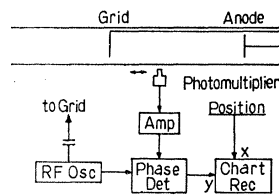


FIG. 3. Block diagram for measurement of the wavelength by means of phase-sensitive detection.

²⁰ M. D. Gabovich, L. L. Pasechnik, and V. G. Yazeva, Zh. Eksperim. i Teor. Fiz. **38**, 1430 (1960) [English transl.: Soviet Phys.—JETP **11**, 1033 (1960)].

²¹ T. Itoh, J. Phys. Soc. Japan **18**, 1695 (1963).

which seems rather smaller than expected. The translation of E/p into the electron drift velocity is made according to empirical data. (See Fig. 4.)^{22,23}

IV. EXPERIMENTAL RESULTS

A. Dispersion Relation of Ion Waves

The experimental confirmation of the dispersion relation for ion waves is shown. Typical examples of spectrum analysis are given in Fig. 5, where Fig. 5(a) is an oscillogram of the panoramic spectrum analyzer and Fig. 5(b) is an X - Y recorder chart from the level meter.

The properties of the spectrum are as follows:

- The fundamental frequency is inversely proportional to the anode-grid distance, L_{AG} .
- The fundamental frequency is independent of the discharge current and the cathode-anode or cathode-grid distances.
- The heater current of the cathode does not affect the spectrum.
- In the low-frequency region, the frequency difference between two neighboring spectra is almost constant and is equal to the fundamental frequency.
- The frequency difference decreases for higher-frequency components.
- The deviation of the frequency difference from the fundamental frequency arises at a lower frequency when the discharge current decreases.
- There exists a distinct cutoff frequency beyond which there are no systematic spectra except for a large oscillation of definite frequency. [Fig. 5(a)]. The cutoff frequency f_c is proportional to the square root of the discharge current and is independent of L_{AG} and the heater current.

The inverse proportionality of the fundamental frequency f_1 to the anode-grid distance seems to be

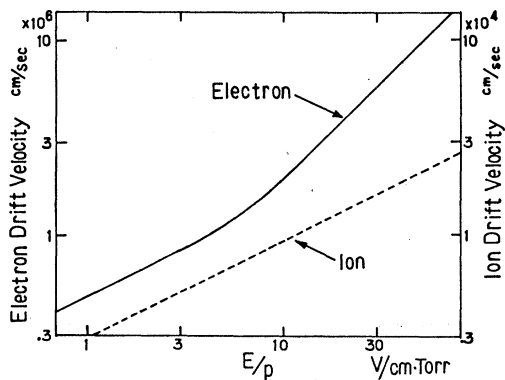
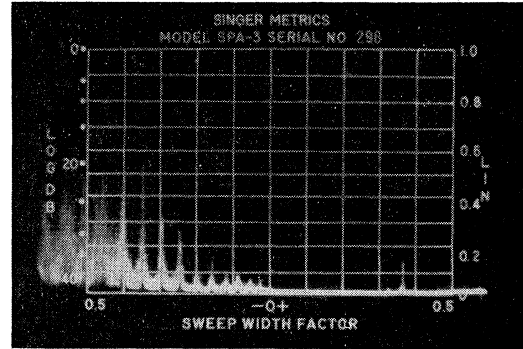


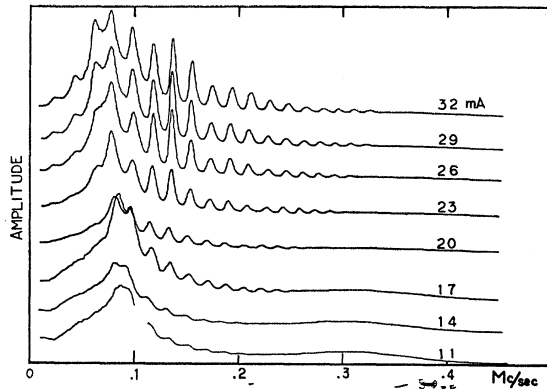
FIG. 4. Electron (solid line) and ion (dotted line) drift velocities in mercury-vapor discharges. (See Refs. 22 and 23.)

²² *Handbuch der Physik*, edited by S. Flügge (Springer-Verlag, Berlin, 1956), Vol. 21.

²³ K. Kingdon and E. Lawton, *Phys. Rev.* **56**, 215 (1939).



(a)



(b)

FIG. 5. (a) Frequency spectra of the anode potential. (Oscillogram obtained by a spectrum analyzer.) Frequency range is 0-1 Mc/sec in full scale. Discharge current is 12 mA. Mercury temperature T_p is 10°C. Anode-grid distance L_{AG} is 1.8 cm. Cutoff frequency appears at about 500 kc/sec. (b) X - Y chart obtained by a level meter. L_{AG} = 4.0 cm. T_p = 29.5°C. The cutoff frequency increases with the root of the discharge current. Amplitude is in arbitrary scale. See Fig. 7.

explained by assuming ion acoustic standing waves between the grid and the anode, the fundamental wavelength of which should be $2 \times L_{AG}$. However, the measurement of wavelength using the phase-sensitive detection always reveals that the wavelength corresponding to the fundamental frequency f_1 is just the anode-grid distance L_{AG} . The phase velocity of the ion acoustic wave becomes $V_s = f_1 \times L_{AG} = 8.0 \pm 0.5 \times 10^4$ cm/sec, which is almost independent of the discharge current.

The fundamental wavelength L_{AG} can be explained as follows. As was shown in Sec. II, only the waves propagating from grid to anode are enhanced. In the plasma, by an unknown mechanism to be discussed later, an instantaneous feedback from anode to grid, or vice versa, occurs, keeping the phase of the waves the same at the anode and grid. (Such a feedback was noted in our previous observations on ion waves.^{24,25}) There-

²⁴ M. Hagi, A. Hirose, and H. Tanaka, *J. Phys. Soc. Japan* **20**, 2307 (1965).

²⁵ A. Hirose, M. Koganei, and H. Tanaka, *J. Phys. Soc. Japan* **21**, 806 (1966).

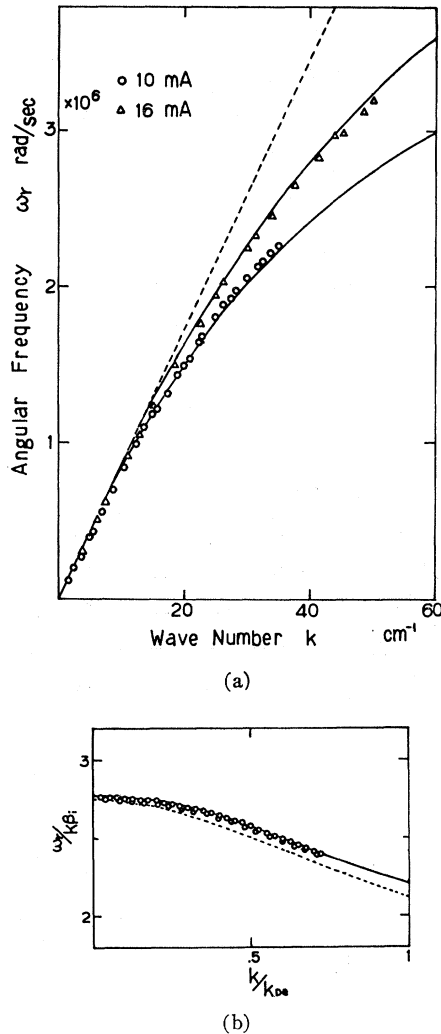


FIG. 6. (a) Dispersion relation at $T_p=14.5^\circ\text{C}$. (k - ω diagram) solid lines come from the simple dispersion relation, Eq. (1), for respective discharge currents. ($\gamma_e=1$ and $\gamma_i=3$.) $k_{De}=60\text{ cm}^{-1}$ for $I_d=10\text{ mA}$ and $k_{De}=78\text{ cm}^{-1}$ for $I_d=16\text{ mA}$. (b) Phase velocity (in the unit of ion thermal velocity) plotted against wave number (in the unit of electron Debye wave number). Solid line is calculated from the Landau dispersion equation, Eq. (8), and dotted line from the fluid model, Eq. (1), with $\gamma_e=1$ and $\gamma_i=3$.

fore, instead of standing waves composed of two counter-directed waves, only the one-way propagating waves satisfying the "same phase condition" $V_s=f_n \times L_{AG}/n$ for $n=1, 2, 3, \dots$, are observed.

The spectrum properties (e) and (f) above represent the dispersion of the waves, indicating that the phase velocity decreases with the frequency. The n th wave number k_n corresponding to the n th spectrum component f_n , is given by $k_n=2\pi n/L_{AG}$. Then, the relation between k_n and $\omega_n(=2\pi f_n)$ is obtained as a k - ω diagram in Fig. 6(a). Low-frequency waves propagate with an almost constant velocity, the so-called ion acoustic wave velocity. The phase velocity of the waves decreases as the frequency increases, thus deviating from the ion

acoustic velocity. The solid curves are obtained from the simple fluid model [Eq. (1)] using the plasma density measured by probes. The temperature ratio T_e/T_i is chosen as 12 for a reason to be explained later. The dispersion of the waves is well demonstrated. The dependence of dispersion on discharge current disappears if the wave number k is normalized by the Debye wave number k_{De} . (The agreement of theory with experiment at each current assures, in turn, such a normalization. Normalization by the ion plasma frequency ω_{pi} and Debye wave number k_{De} is used hereafter.)

For a comparison with the more exact theory, i.e., Eq. (8), the normalized wave number-velocity ($k/k_{De}-\omega/k\beta_i$) diagram is shown in Fig. 6(b), where the solid line comes from the Landau dispersion equation for $T_e/T_i=12$. This line is insensitive to the electron drift velocity in our experimental range. For reference, the dotted line is calculated from the fluid model Eq. (1) with $\gamma_e=1$ and $\gamma_i=3$. As the estimation of the wave velocity may contain errors of about $\pm 5\%$, there is no practical difference between two theoretical results.

B. Dependence of Cutoff Frequency on Electron Drift

The cutoff wave number is compared with the theoretical stable-unstable boundary described in Sec. II. Using the cutoff phenomenon in the dispersion relation of ion waves, we investigate the mechanism which sustains ion waves in the discharges. In our previous paper,¹⁵ it was reported that the cutoff frequency f_c equals $f_{pi}/\sqrt{2}$ or, in terms of the wavelength, the cutoff wavelength is $2\pi\lambda_D$, where λ_D is the electron Debye length. This interesting result is only partially correct, because the cutoff frequency strongly depends on electron drift velocity. Our previous result corresponds to a rather large electron drift velocity (low mercury

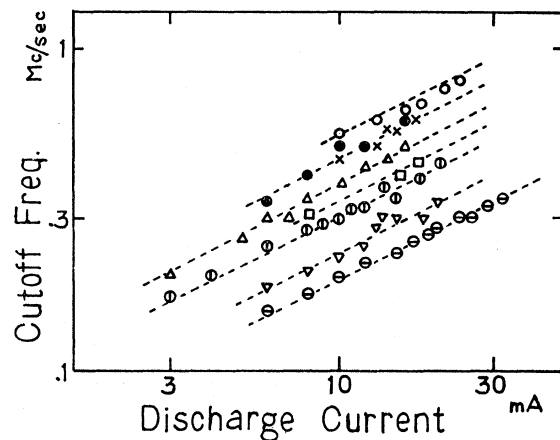


FIG. 7. Variation of cutoff frequency due to the mercury-pool temperature. $\circ=6^\circ\text{C}$, $\times=8^\circ\text{C}$, $\bullet=10^\circ\text{C}$, $\Delta=14.5^\circ\text{C}$, $\square=18^\circ\text{C}$, $\oplus=23^\circ\text{C}$, $\nabla=26^\circ\text{C}$, $\ominus=29.5^\circ\text{C}$. At each temperature, the cutoff frequency increases with the root of the current or the density.

vapor pressure). Let us now summarize the properties of the cutoff.

(a) At each electron drift velocity (mercury vapor pressure), the cutoff frequency f_c is always proportional to the root of the plasma density (discharge current) (Fig. 7). Therefore, the normalized cutoff frequency ω_c/ω_{pi} is useful in the following analysis.

(b) The normalized cutoff frequency ω_c/ω_{pi} decreases with the mercury vapor pressure (Fig. 8).

(c) The heater current and the anode-grid distance are not responsible for the cutoff.

(d) The cutoff appears very distinctly.

An abrupt disappearance of higher modes strongly suggests that a stable-unstable boundary exists in the vicinity of the cutoff frequency or the cutoff wave number. For the convenience of theoretical discussion, the cutoff frequency ω_c/ω_{pi} is translated into the cutoff wave number k_c/k_{De} , either by direct measurement or by means of the dispersion relation. Thus, the cutoff wave

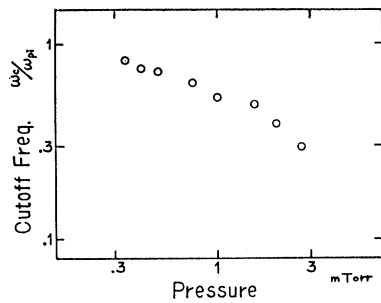


FIG. 8. Translation of Fig. 7. Cutoff frequency is expressed in the unit of ion plasma frequency to eliminate the discharge current.

number k_c/k_{De} is plotted against the electron drift velocity. (Fig. 9).

The solid line in Fig. 9 indicates the theoretical stable-unstable boundary, calculated from the Landau dispersion equation, corresponding to the temperature ratio $T_e/T_i=12$ as a best fit. Though the ion temperature T_i is not measured directly, the agreement of theory with experiment will provide a satisfactory demonstration of the drift instability of two-Maxwellian-component plasma.⁸ The ion waves are enhanced by the relative drift velocity between electrons and ions. More precisely, a doubly-humped distribution function⁷ (f_e+f_i) makes the waves grow against the Landau damping which might have depressed any longitudinal waves in the absence of drift velocity.

C. One-Way Propagation of Ion Waves (External Excitation)

According to theory (Sec. II), only the waves in the direction of the electron drift are enhanced if the ion drift velocity is smaller than the wave velocity. The result that the fundamental wavelength is L_{AG} instead

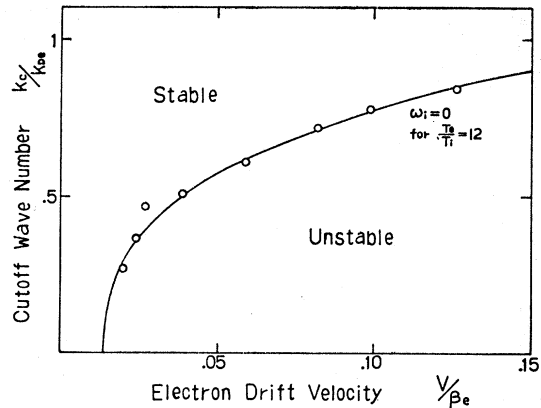


FIG. 9. Stable-unstable boundary experimentally obtained (circle). Solid line represents the theoretical boundary for $T_e/T_i=12$.

of $2L_{AG}$ (as discussed in Sec. IV A) may be a partial confirmation of this one-way propagation. For a direct confirmation of this statement, the propagation of externally excited ion waves has been examined by means of phase-sensitive detection (Fig. 3). For this purpose, the spontaneously excited waves have to be eliminated from the measurement of the propagation waves. The former disappear when the separation of grid and anode, L_{AG} , becomes more than 10 cm.

The grid is used as an exciter, and two typical results are shown in Fig. 10. Cathode-directed waves suffer a strong damping and are hard to detect. On the other hand, anode-directed waves can propagate safely even though they also experience appreciable damping. However, a quantitative discussion of damping rate would be inadequate under our present experimental conditions.

V. DISCUSSIONS

As stated in the previous sections, the prediction of the Landau dispersion equation [Eq. (8)] is experimentally confirmed. This equation was derived from the collisionless Vlasov equation. In our plasma, how-

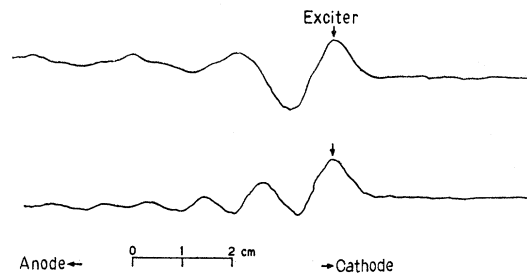


FIG. 10. Examples of demonstrating the one-way propagation of the ion acoustic waves. Output from the phase-sensitive detector is traced against the axial position of photomultiplier (cf. Fig. 3). ↓ shows the position of the exciting grid, and only anode directed waves can propagate though they experience damping. Cathode-directed waves are not detected. Exciting frequency is 40 kc/sec for the upper and 67 kc/sec for the lower.

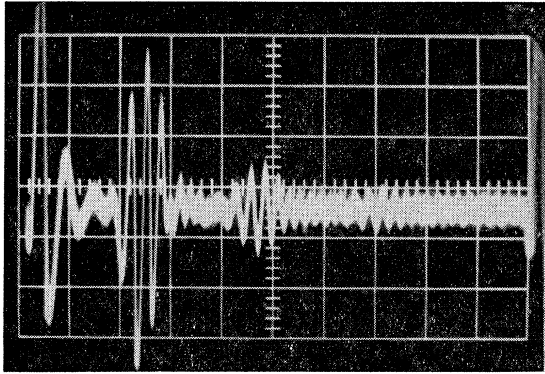


FIG. 11. Oscilloscope of the anode potential when a pulse is supplied to the anode. $L_{AG}=5.4$ cm. The time scale is $30 \mu\text{sec}/\text{division}$.

ever, the electron-neutral collision frequency is of the order 10^6 – 10^7 , and the effect of such collision on the damping of the waves seems to be very important. Fortunately, it is proved,²⁶ by numerical calculation, that electron-neutral collision scarcely affects the cutoff frequency when the electron drift is rather small, as is so in our case. Our cutoff is, therefore, almost due to the collisionless damping.

In our observation of ion waves spontaneously excited between the electrodes, the measurements of the growth or damping rate was impossible. Signals arrive at the anode, and by an unknown mechanism they are instantaneously fed back to the grid in the plasma column. This feedback mechanism, probably of electrostatic nature,^{27,28} keeps the ion waves the same at both electrodes. This is why the standing-wave type of resonance relation, $V_s = f_n \times L_{AG}/n$ ($n=1, 2, \dots$) is observed for spontaneously excited and one-way propagating waves. The anode and the grid, in a certain sense, are short-circuited and only the waves satisfying the above relation are observed, others being damped by interferences due to phase randomization. This sort of behavior may be related to our previous observation that the plasma column oscillates as a whole when rf signals are supplied at the grid or the anode.^{24,25} The spontaneously excited ion waves themselves have the same effect on the plasma column. Therefore, without the method of phase-sensitive detection, the photomultiplier's output shows no phase difference among oscillations measured at different axial positions. This means that the plasma column is oscillating as a whole at the same frequency as that of the propagating ion waves. In our previous experiments on ion wave propagation, we had obtained Fig. 11 as an example of multiple reflections of ion waves.²⁹ This is an oscilloscope

of the anode potential when a pulse is supplied at the anode. We had interpreted Fig. 11 as multiple reflections of ion wave pulses between the grid and the anode. This is not correct, however, based on our present knowledge of the one-way propagation of the ion waves. The second pulse in Fig. 11 was previously considered to have traveled from the anode to the grid and back again towards the anode, being reflected at the grid. However, only propagation of ion waves from the grid to the anode is possible under the present conditions. When the first pulse is supplied at the anode, a pulse signal instantaneously appears at the grid (feedback mechanism) and it travels towards the anode arriving as the second pulse. Next, the arrival of the second pulse at the anode again gives rise to a pulse at the grid which will appear as the third pulse after propagation, with the velocity of the ion acoustic waves, and so on. Simply, it is a repetition of one-way propagation and not the presumed multiple reflections of the pulses. The mechanism of such an instantaneous feedback between electrodes in the plasma is not yet known.

In the present experiment on ion wave instabilities, the temperature ratio T_e/T_i appears as a prominent parameter in determining the stable-unstable boundary. The electron temperature T_e is directly measured by the probe, while the ion temperature T_i is very hard to measure in a simple way. From the relation between the cutoff wave number and the electron drift velocity, we experimentally obtained the ratio $T_e/T_i=12$ as the best fitting value. However, the electron drift velocity is estimated as a function of E/p , where the electric field E (of the order 0.01 V/cm) is measured by the probe. Taking into account inevitable errors in the measurements of the electric field, the experimental fit would be tolerable for $T_e/T_i=10$ – 15 . In spite of clear cutoff phenomena shown in Fig. 5, such uncertainty is inevitable because the electron drift velocity is estimated from the internal electric field. The velocity of the ion acoustic waves can be measured with considerable accuracy and one might expect to be able to determine the ion temperature from the fluid theory relation, $V_s = [(T_e + 3T_i)/M]^{1/2}$. However, the uncertainty in the measurement T_e makes it difficult to estimate the ion temperature from the above relation. Furthermore, the dispersion relation from kinetic theory [the solution of Eq. (8) for ω_r] is not too sensitive to the ratio T_e/T_i , so that the experimental choice of a particular value of T_e/T_i is not very exact. Recently, it has been reported that the ion temperature in a low-pressure mercury-vapor discharge is quite high ($T_i=2150^\circ\text{K}$).³⁰ Such a high ion temperature is understandable, if collisions between ions and neutral atoms are not so frequent as to thermalize the ions. The collision frequency ν_{in} (ion-neutral) is of order $5 \times 10^8/\text{sec}$ and the mean free path of the ion is comparable with the

²⁶ H. Momota, S. Ohuchi, and J. Washimi, in the 22nd Conference of the Physical Society of Japan, 1967 (unpublished).

²⁷ E. B. Armstrong, K. G. Emeleus, and T. R. Neil, Proc. Roy. Irish Acad. **A54**, 291 (1951).

²⁸ I. Alexeff and W. D. Jones, Phys. Rev. Letters **15**, 286 (1965).

²⁹ H. Tanaca and M. Hagi, Phys. Fluids **9**, 222 (1966).

³⁰ N. Ionov and A. Y. Tontegode, Zh. Tekhn. Fiz. **34**, 354 (1964) [English transl.: Soviet Phys.—Tech. Phys. **9**, 279 (1964)].

diameter of the discharge tube. We may therefore say that the collisions between ions and neutrals are rare and the ion temperature would be higher than the neutral gas temperature.

The ion drift velocity, which might be of the order of 10% of the phase velocity of the ion waves, has been neglected in the experimental analysis. Under our experimental condition, where only anode-directed waves are observed, the detection of the Doppler effect due to ion drift velocity is not observed. The effect of the ion drift velocity will be discussed in our next experiment of the damping and growth rates of ion waves.

We may add a remark on the ion-plasma oscillations. As was already reported,¹⁵ the distinct oscillation beyond the cutoff frequency [see Fig. 5(a)] may be considered as the ion-plasma oscillation because its frequency almost satisfies the relation $\omega^2 = 4\pi ne^2/M$, where n is the electron density measured by the probe. However, we have no adequate experimental basis to distinguish it from the so-called potential-minimum oscillation.³¹ The electron density n in the experimental analysis is estimated from the dispersive behavior of the waves, and neither this "ambiguous" ion-plasma frequency nor the information from the Langmuir probe is used. The Langmuir probe reveals that a strong radial dependence of the electron density is present in the discharge tube. However, the value at the axial center is most consistent with the experimental dispersion relation. The spontaneous waves, therefore, seem to be excited near the central axis of the tube, and the cross section responsible for the enhancement of the waves may be very small. In such a case, the simplified one-dimensional theory may be very applicable to the analysis. On the other hand, in the case of the external excitation, the waves will be emitted from the full surface of the grid which is almost half the size of the tube in diameter. Therefore, the one-dimensional approach will not be adequate because of the nonuniformity of the density and the finite dimension of the plasma.

Concerning the cutoff frequency, it should be noted that the waves in our experiment are spontaneously excited in a plasma because of a relative drift velocity

³¹ F. W. Crawford, *J. Appl. Phys.* **33**, 15 (1962).

between ions and electrons. Under our experimental conditions, at rather a high ion temperature, the cutoff always occurs under the ion-plasma frequency.^{15,32} Recently, the propagation of externally excited waves of frequency much higher than the ion-plasma frequency has been reported.³³ In this case, the electron thermal motion plays an important role in sustaining the propagation of such high-frequency waves. Further, this propagation is observed in a quiescent plasma. Therefore, our cutoff in the self-excitation of the waves in a drifting plasma does not concern the external excitation of waves by a dipole grid.^{34,35}

Finally, we may add a remark on the compressional coefficients γ_e and γ_i . In the absence of an external magnetic field, the experimental requirement for $\gamma_e=1$ has been reported.²⁸ In our case, too, $\gamma_e=1$ is experimentally obtained, which is a reasonable prediction from the kinetic theory. This means that the electrons contribute to the waves as an electron fluid background.³⁶ On the other hand, there has been no experimental report on γ_i . However, as stated in Sec. IV, our observation on the dispersion relation requires $\gamma_i=3$, which agrees with theoretical expectation in the one-dimensional approach. γ_e and γ_i in a magnetic field are under detailed study, and a critical transition from $\gamma_e=1$ to $\gamma_e=3$ is observed.³⁷

Our results on the cutoff frequency in the dispersion relation can be safely considered as an experimental confirmation of the Landau dispersion equation.

The ion waves in an external magnetic field are under examination.

ACKNOWLEDGMENTS

The authors would like to express their thanks to Professor K. Takayama and Dr. H. Momota of the Institute of Plasma Physics, Nagoya University, for stimulating discussions.

³² I. Alexeff and W. D. Jones, in *Proceedings of the Seventh International Conference on Ionization Phenomena in Gases*, Belgrade, 1965 (unpublished).

³³ G. M. Sessler, *Phys. Rev. Letters* **17**, 243 (1966).

³⁴ R. W. Gould, *Phys. Rev.* **136**, A991 (1964).

³⁵ A. Y. Wong, *Phys. Rev. Letters* **14**, 252 (1965).

³⁶ A. Y. Wong, R. W. Motley, and N. D. D'Angelo, *Phys. Rev.* **133**, A436 (1964).

³⁷ H. Tanaka and A. Hirose (to be published).

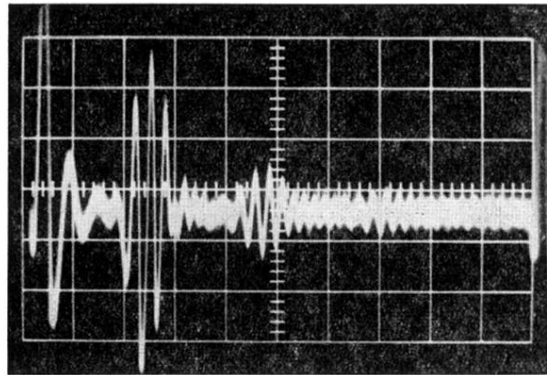
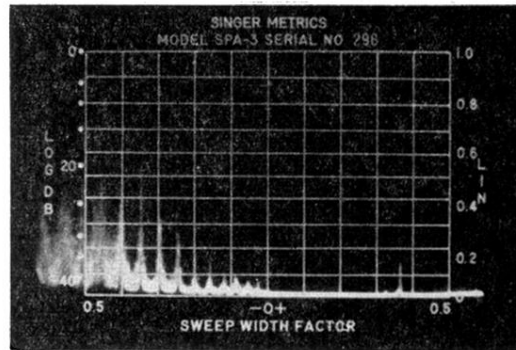
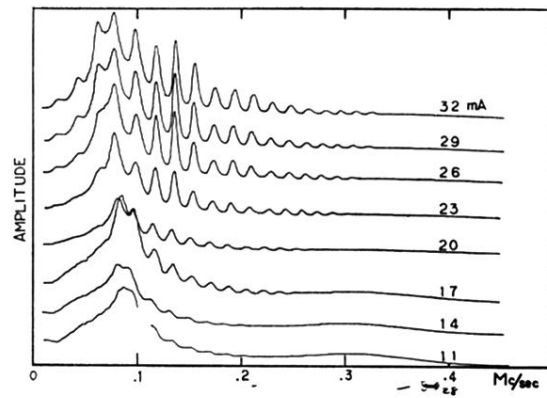


FIG. 11. Oscillogram of the anode potential when a pulse is supplied to the anode. $L_{AG}=5.4$ cm. The time scale is $30 \mu\text{sec}/$ division.



(a)



(b)

FIG. 5. (a) Frequency spectra of the anode potential. (Oscillogram obtained by a spectrum analyzer.) Frequency range is 0–1 Mc/sec in full scale. Discharge current is 12 mA. Mercury temperature T_p is 10°C. Anode-grid distance L_{AG} is 1.8 cm. Cutoff frequency appears at about 500 kc/sec. (b) X-Y chart obtained by a level meter. L_{AG} = 4.0 cm. T_p = 29.5°C. The cutoff frequency increases with the root of the discharge current. Amplitude is in arbitrary scale. See Fig. 7.